Supporting Information

Graphene-Enabled, Spatially Controlled Electroporation of Adherent Cells for Live-Cell Super-Resolution Microscopy

Seonah Moon[†,#], Wan Li[†,#], Meghan Hauser[†], Ke Xu[*,†,‡]

[†]*Department of Chemistry, University of California, Berkeley, CA 94720*

[‡]*Chan Zuckerberg Biohub, San Francisco, CA 94158*

[#]*These authors contributed equally*

* xuk@berkeley.edu

Supplementary Figures

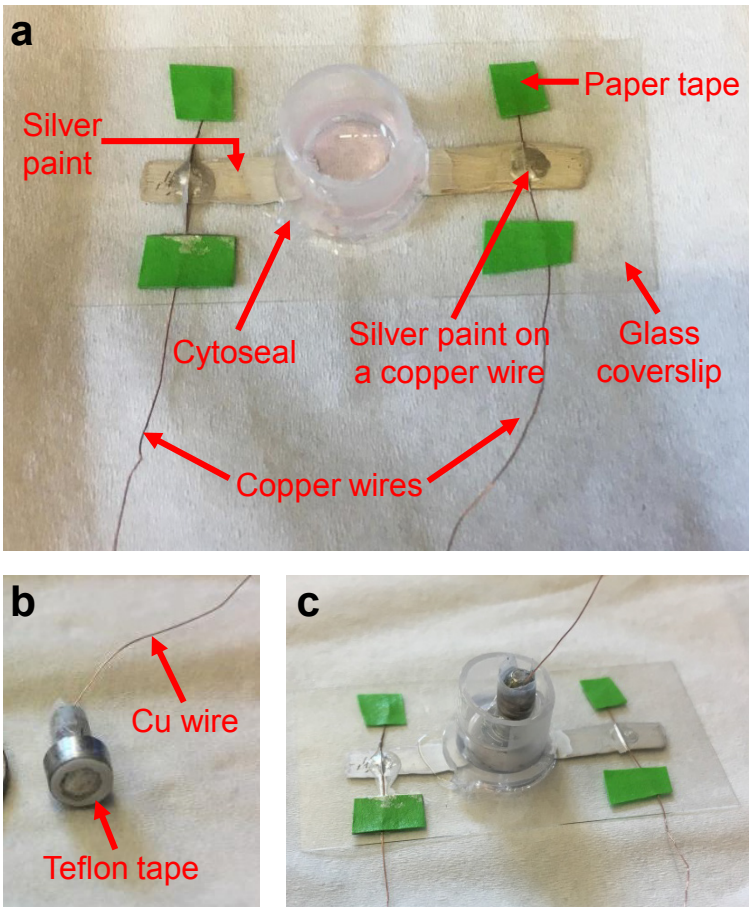

Figure S1. Photographs of the device. (a) The assembled device without the metal counter electrode. (b) The metal counter electrode, made out of a metal pin-stub mount commonly used in scanning electron microscopy. (c) The completed device with the counter electrode.

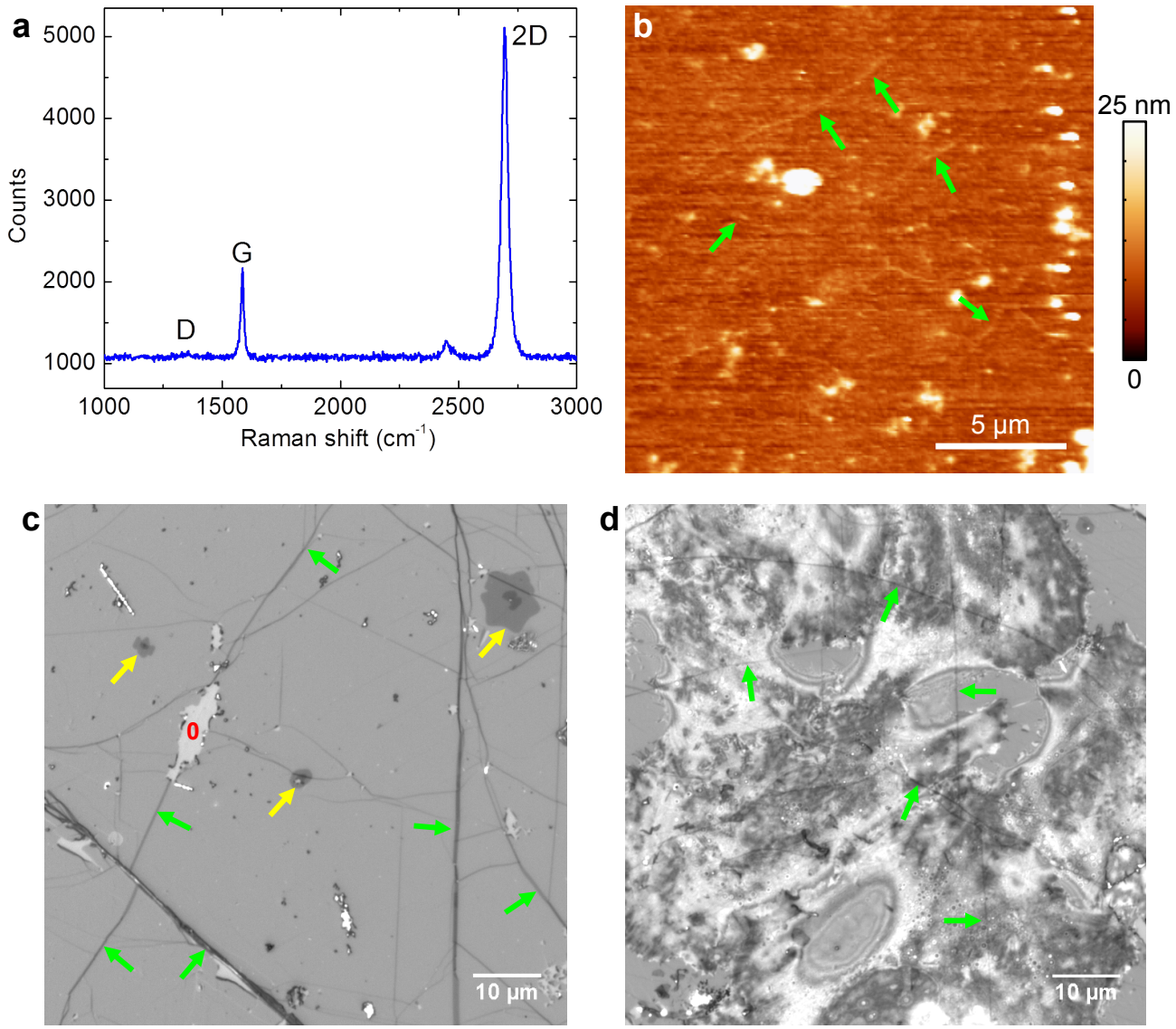

Figure S2. Characterization of the graphene sheets used in the experiment. (a) Raman spectroscopy of the graphene sheet deposited on a glass coverslip, indicating that the graphene was dominantly monolayer with a low defect level. (b) AFM image of the graphene surface. Green arrows point to typical wrinkles in the graphene sheet. (c,d) IRM images of the fully assembled graphene electroporation device, after culturing 24 h, for an area without cell coverage (c) and an area with cell coverage (d), respectively. Green arrows point to wrinkles in graphene. "0" in (c) marks a small region of exposed glass surface due to a hole in the otherwise continuous graphene monolayer. Yellow arrows in (c) point to sporadic, micrometer-scale islands of bilayers on the graphene monolayer. See detailed interpretation of IRM data for graphene in Ref 1, as well as for adherent cells in Refs 2,3.

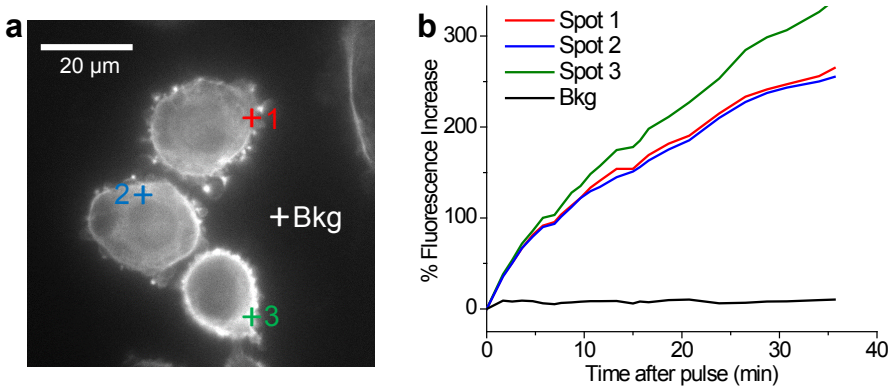

Figure S3. Labeling results over longer time scales. (a) Fluorescence micrograph for the graphene-electroporation delivery of phalloidin-AF488 in to A549 cells, at 36 min after the voltage pulse. (b) Change in local fluorescence intensity over time after the voltage pulse, for the different spots marked in (a).

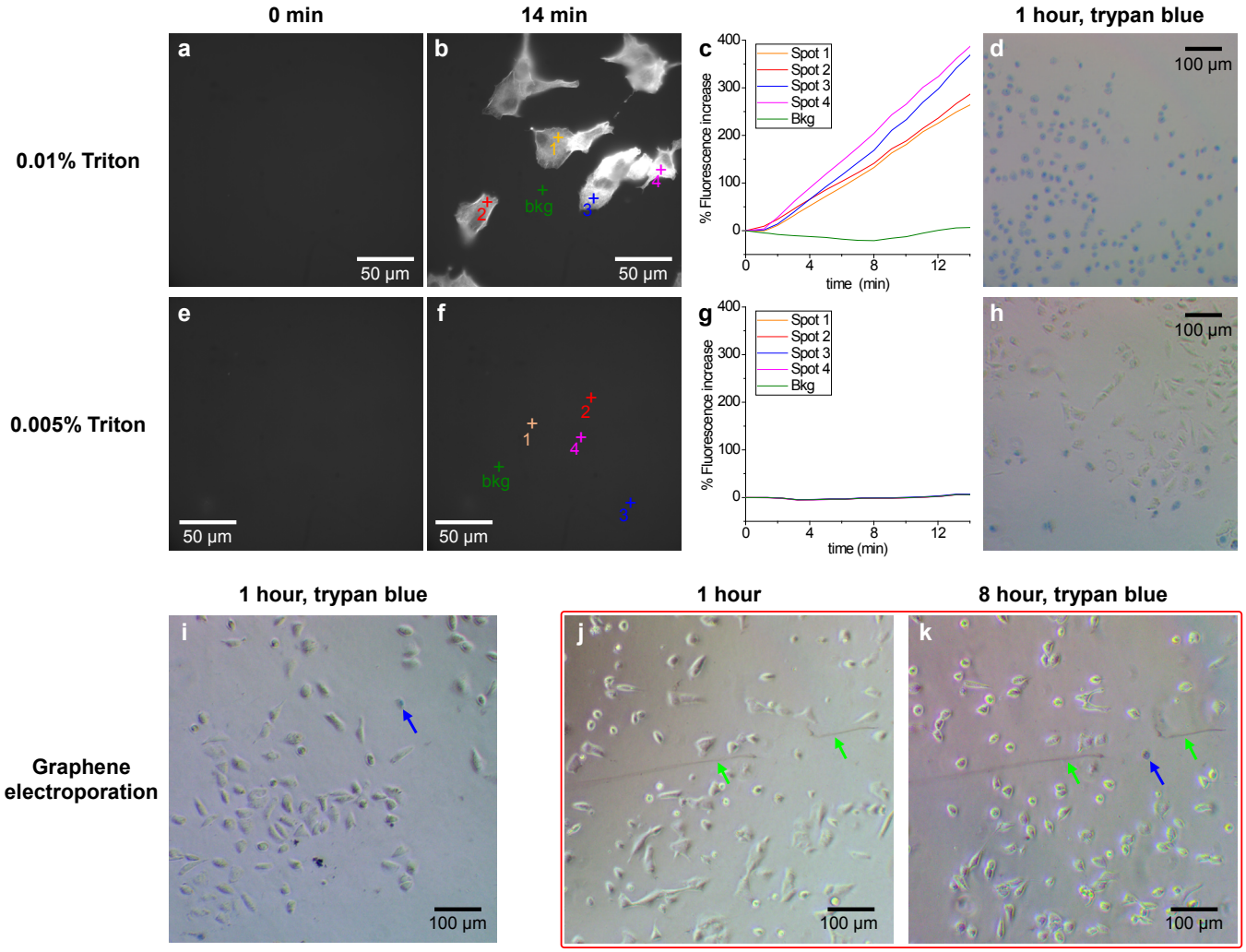

Figure S4. Cell viability tests for cells after Triton treatment vs. cells after graphene-based electroporation. (a,b) Fluorescence micrographs for the delivery of phalloidin-AF488 into A549 cells through the addition of 0.01% Triton X-100 into the medium at 0 min (a) and 14 min (b), respectively. (c) Change in local fluorescence intensity over time, for the different spots marked in (b): Spots 1-4 are on cells, whereas "bkg" corresponds to the background. (d) Trypan blue assay for the Triton-treated cells after recovery in the incubator for 1 h. All cells in the view were stained, indicating cell death. (e,f) Fluorescence micrographs for the delivery of phalloidin-AF488 into another sample through the addition of 0.005% Triton X-100 into the medium at 0 min (e) and 14 min (f), respectively. (g) Change in local fluorescence intensity over time, for the different spots marked in (f): Spots 1-4 are on cells, whereas "bkg" corresponds to the background. (h) Trypan blue assay for the Triton-treated cells after recovery in the incubator for 1 h. A fraction of the cells were stained, indicating that some cells died, even though most cells are not yet labeled by phalloidin-AF488 at this lower Triton concentration, as suggested by (e-g). (i) Trypan blue assay for A549 cells after graphene-based electroporation and recovery in the incubator for 1 h. Blue arrow points to a cell that is stained, whereas most other cells are not stained. (j,k) Another sample after graphene-based electroporation and recovery in the incubator for 1h (j), as well as trypan blue assay after further incubating for an additional 7 h in the incubator. Blue arrow points to a cell that is stained. Other cells in the view are not stained, and the cell shapes changed substantially between 1 and 8 h, thus further indicating cell viability. Green arrows point to major wrinkles in graphene, which helped in aligning the two images.

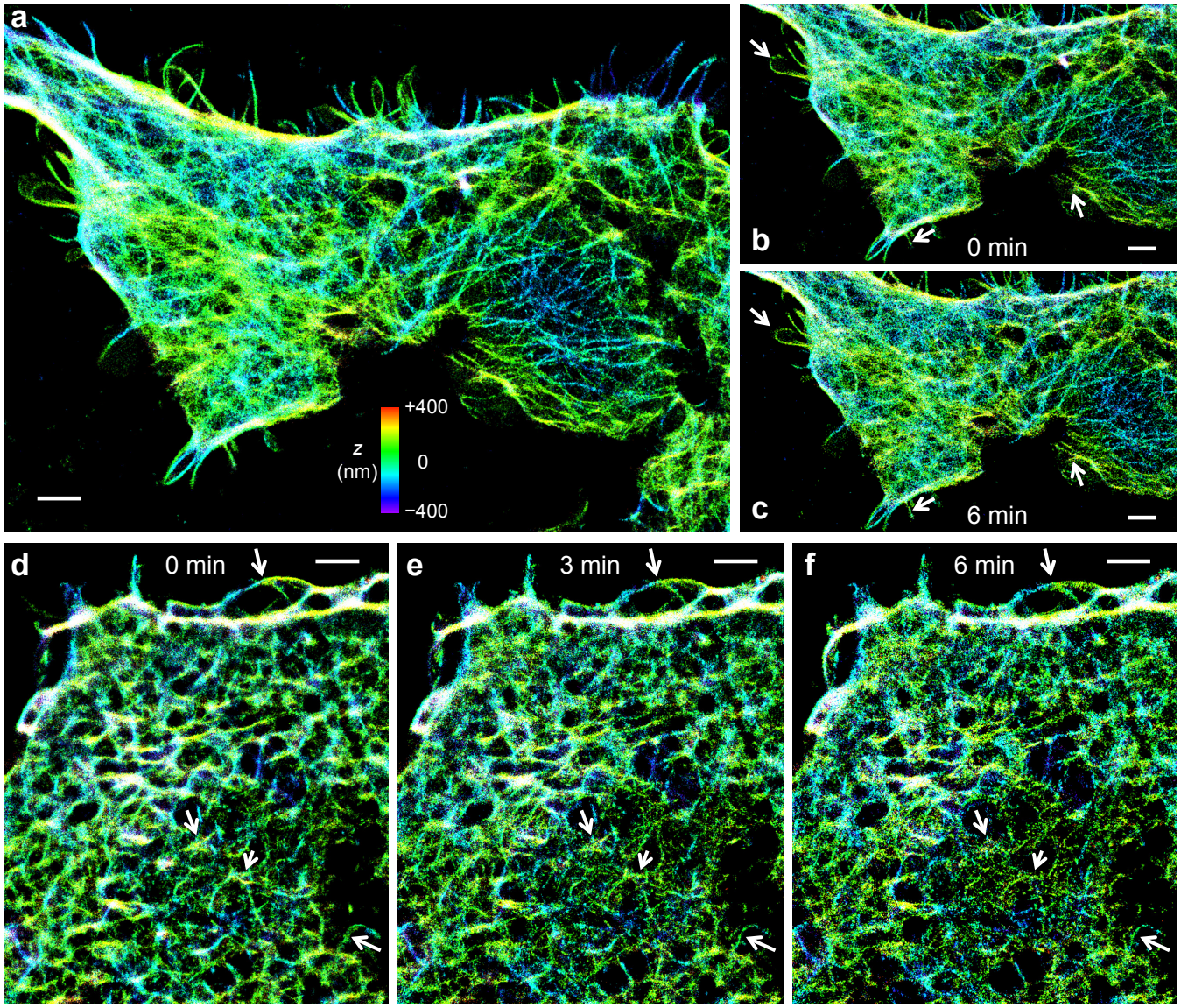

Figure S5. 3D-STORM SRM of the actin cytoskeleton in live A549 cells labeled through the graphene-electroporation delivery of phalloidin-AF647. (a) 3D-STORM image of one cell, obtained by integrating frames of single-molecule images over 10 min. (b,c) 3D-STORM images for a region of the sample, obtained by integrating frames over 0-3 min (b) and 6-9 min (c). (d-f) A sequence of 3D-STORM images for another sample, obtained by integrating frames over 0-3 min (d), 3-6 min (e), and 6-9 min (c). Arrows point to structural changes at the nanoscale. Scale bars: 2 μm.

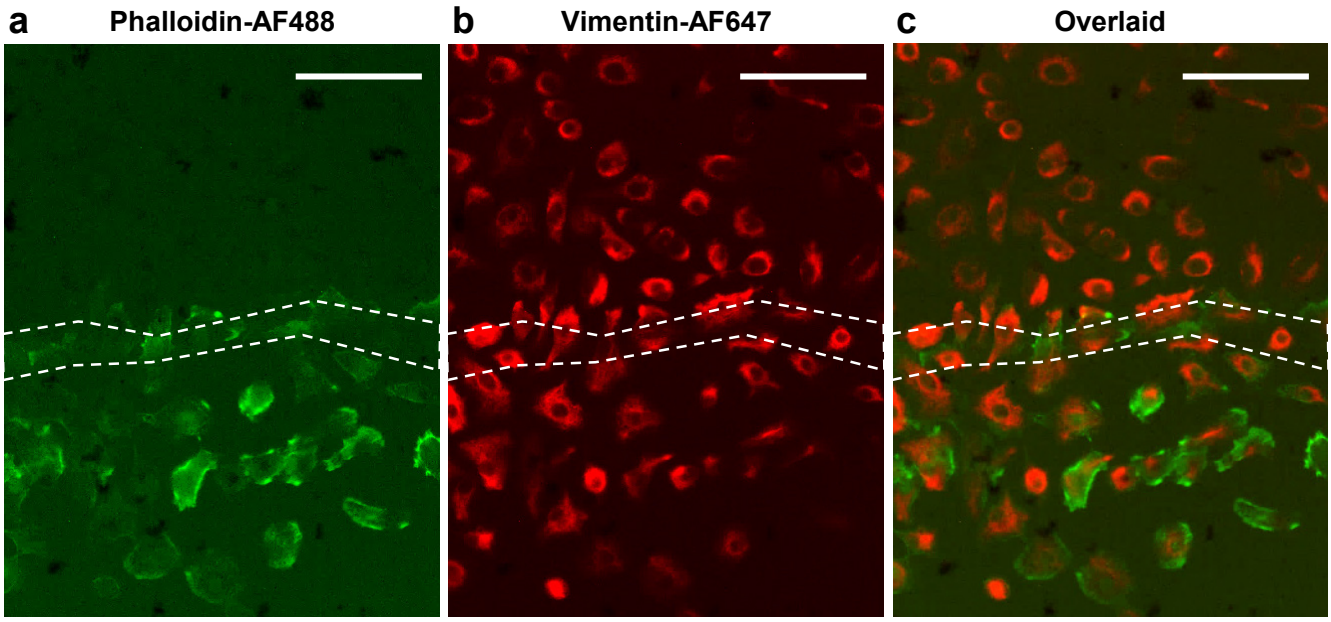

Figure S6. Incomplete recovery of the plasma membrane led to unspecific delivery of the second probe. Here, electroporation was first performed for the bottom half of the graphene electrode in a phalloidin-AF488-loaded electroporation buffer. The sample was incubated for 2 min and 15 min in the electroporation buffer and regular culture medium, respectively, and then electroporation was performed for the top half in another electroporation buffer loaded with AF647-tagged anti-vimentin IgG. (a) Fluorescence micrograph for the first probe (phalloidin-AF488). (b) Fluorescence micrograph for the second probe (AF647-tagged anti-vimentin IgG). (c) Overlay of the two color channels. Dashed lines mark the edges of the top and bottom electrodes. Scale bars: 50 μm. Whereas delivery of the first probe was specific to the bottom half of the device (a), delivery of the second probe was not specific to the top half of the device (b), as cells on the bottom half had not fully sealed their plasma membrane when the second probe was added.

Reference for Supporting Information

(1) Li, W.; Moon, S.; Wojcik, M.; Xu, K. Direct Optical Visualization of Graphene and Its Nanoscale Defects on Transparent Substrates. *Nano Lett.* **2016**, *16*, 5027-5031.

(2) Curtis, A. S. G. The Mechanism of Adhesion of Cells to Glass: A Study by Interference Reflection Microscopy. *J. Cell Biol.* **1964**, *20*, 199-215.

(3) Verschueren, H. Interference Reflection Microscopy in Cell Biology: Methodology and Applications. *J. Cell Sci.* **1985**, *75*, 279-301.